Hydrolysis of the Borohydride Anion BH4–: A 11B NMR Study Showing the Formation of Short-Living Reaction Intermediates including BH3OH–

Eddy Petit, Fabrice Salles, Damien Alligier, Umit Demirci

Article

Hydrolysis of the Borohydride Anion BH_4^-: A ^{11}B NMR Study Showing the Formation of Short-Living Reaction Intermediates including BH_3OH^-

Eddy Petit [1] , **Fabrice Salles [2]** , **Damien Alligier [1] and Umit B. Demirci [1],***

[1] Institut Européen des Membranes, IEM—UMR 5635, ENSCM, CNRS, University Montpellier, 34095 Montpellier, France; eddy.petit@umontpellier.fr (E.P.); alligier.damien@gmail.com (D.A.)

[2] ICGM, University Montpellier, CNRS, ENSCM, Montpellier, France; fabrice.salles@umontpellier.fr

* Correspondence: umit.demirci@umontpellier.fr

Abstract: In hydrolysis and electro-oxidation of the borohydride anion BH_4^-, key reactions in the field of energy, one critical short-living intermediate is BH_3OH^-. When water was used as both solvent and reactant, only BH_3OH^- is detected by ^{11}B NMR. By moving away from such conditions and using DMF as solvent and water as reactant in excess, four ^{11}B NMR quartets were observed. These signals were due to BH_3-based intermediates as suggested by theoretical calculations; they were DMF·BH_3, BH_3OH^-, and $B_2H_7^-$ (i.e., $[H_3B-H-BH_3]^-$ or $[H_4B-BH_3]^-$). Our results shed light on the importance of BH_3 stemming from BH_4^- and on its capacity as Lewis acid to interact with Lewis bases such as DMF, OH^-, and BH_4^-. These findings are important for a better understanding at the molecular level of hydrolysis of BH_4^- and production of impurities in boranes synthesis.

Keywords: borate; borohydride; hydrogen; hydrolysis; short-living intermediates

1. Introduction

Sodium borohydride $NaBH_4$ in alkaline aqueous solution is a potential fuel of low-temperature fuel cell [1]. It is regarded as an *indirect* fuel (i.e., H carrier) when it is hydrolyzed to produce H_2, the as-produced H_2 then feeding a fuel cell (Equation (1)) [2]. It is regarded as a *direct* fuel (i.e., reductant) when it directly feeds a direct liquid fuel cell to be electro-oxidized (Equation (2)) [3]:

$$BH_4^- \text{ (aq)} + 4H_2O \text{ (l)} \rightarrow B(OH)_4^- \text{ (aq)} + 4H_2 \text{ (g)} \tag{1}$$

$$BH_4^- \text{ (aq)} + 8OH^- \text{ (l)} \rightarrow B(OH)_4^- \text{ (aq)} + 4H_2O \text{ (l)} + 8e^- \tag{2}$$
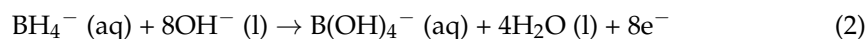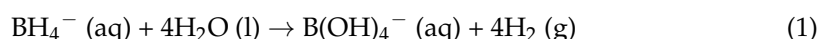
The aqueous solution has to be alkaline, that is, stabilized [4], because this is the only way to prevent spontaneous (exothermic, with an enthalpy of about -240 kJ mol^{-1} [5]) hydrolysis of BH_4^- from occurring extensively. In hydrolysis (Equation (1)), a metal catalyst is therefore required to accelerate the production of H_2 [6]. In electro-oxidation (Equation (2)), a metal electro-catalyst is required to promote the generation of a maximum of electrons (out of eight) [4]. However, the electro-catalyst also acts as catalyst of hydrolysis, a reaction that is in this case regarded as heterogeneous because it is detrimental to the fuel cell faradaic efficiency [7].

In hydrolysis (Equation (1)) as well as in electro-oxidation (Equation (2)), complete reaction implies transformation of BH_4^- into $B(OH)_4^-$ via formation of short-living intermediates. For spontaneous hydrolysis, Mochalov et al., suggested in 1965 BH_3OH^-, $BH_2(OH)_2^-$, and $BH(OH)_3^-$ as possible short-living intermediates [8]. They showed, for instance, that the direct transformation of BH_4^- into $B(OH)_4^-$ has the same kinetic constant ($k = 5.31 \times 10^7$ min^{-1}) as the transformation of BH_4^- into BH_3OH^- ($k' = 5.15 \times 10^7$ min^{-1}). The same year, Gardiner and Collat suggested the formation of BH_3, BH_3OH^-, and

[H]$^+$[BHOH]$^-$ as possible short-living intermediates [9]. More recently, Guella et al. reported that, by ^{11}B nuclear magnetic resonance (NMR) spectroscopy, they detected only BH$_4^-$ and B(OH)$_4^-$ (Equation (1)) for a Pd-catalyzed hydrolysis [10]. The non-detection of other species was explained by the fact that the hydrolysis intermediates are excessively short-living in their experimental conditions. By quantum chemical calculations, Lu et al. [11] confirmed Guella et al.'s explanation and modelled a multistep process involving the following hypothetical short-living intermediates (Equation (3)):

$$BH_4^- \rightarrow BH_3OH^- \rightarrow H_2BO^- \rightarrow BH_2(OH)_2^- \rightarrow HB(O)OH^- \rightarrow BH(OH)_3^- \rightarrow B(O)(OH)_2^- \rightarrow B(OH)_4^- \qquad (3)$$

Comparable predictions were reported by Zhou et al. [12], Andrieux et al. [13], Churikov et al. [14], and Choi et al. [15] detected traces of BH$_3$OH$^-$ by using ^{11}B NMR spectroscopy. It is therefore arguable whether BH$_3$OH$^-$, as the first short-living intermediate, directly hydrolyzes into B(OH)$_4^-$. This is a possible parallel pathway as suggested by Mochalov et al. [8] for example.

Budroni et al. [16] refers to BH$_3$OH$^-$ as a critical short-living intermediate. As discussed above, this applies to the hydrolysis reaction (Equation (1)). Interestingly, this also applies to electro-oxidation of BH$_4^-$ (Equation (2)) on metal electrodes (e.g., Pd, Pt, and Au) [17–23]. For instance, Molina Concha et al. [24] studied Pt-catalyzed electro-oxidation of BH$_4^-$ by in situ Fourier Transform Infrared (FTIR) spectroscopy. They observed that: (i) BH$_3$OH$^-$ formed at low potentials (<0.7 V) by hydrolysis of BH$_4^-$ and/or partial oxidation of BH$_4^-$; (ii) BH$_3$OH$^-$ quickly electro-oxidized into BH$_2$ intermediates such as BH$_2$OH and BH$_2$(OH)$_2^-$; and (iii) the BH$_2$ intermediates electro-oxidized into BO$_2^-$ at high potentials (>0.7 V).

Similarly, Nanayakkara et al. [25] investigated the mechanism of H$_2$ release of BH$_3$ in water and the following solvent effects by using MP2 quantum calculations. One H$_2$O molecule interacting with BH$_3$ led to an activation energy equal to 24.9 kcal mol^{-1}, while the energy values ranged from 29 and 32 kcal mol^{-1} when one H$_2$O molecule interacted with BH$_3$ and another H$_2$O molecule interacted with the H$_2$O molecule bonded to BH$_3$. The resulting enthalpy was estimated at 20 kcal mol^{-1} for the first configuration and ranged between 12 and 14 kcal mol^{-1} for the others.

The present study is to be seen against the background described above. Based on a systematic study using ^{11}B NMR spectroscopy, we attempted to detect and identify any short-living intermediates in order to gain insight and better understanding of both hydrolysis and electro-oxidation of BH$_4^-$. Furthermore, theoretical investigations were performed for obtaining vibrational results, determining the sensitive frequencies and estimating the energies of the different hypothetical molecular structures.

2. Results and Discussion

2.1. Hydrolysis Conditions Where H$_2$O Acts as Both Reactant and Solvent

In hydrolysis and electro-oxidation conditions, the fuel is an alkaline aqueous solution of BH$_4^-$ for which the concentration of BH$_4^-$ is usually kept low (typically < 1 M). We therefore set our experimental conditions to be in line with such practices: the concentration of NaOH was fixed as 0.1 M and the concentration of BH$_4^-$ (from NaBH$_4$) was chosen as 0.66 M.

In hydrolysis and electro-oxidation conditions, the reaction is catalyzed by a metal catalyst and an electro-catalyst, respectively. We selected three bulk metals such as Pd, Pt, and Au (each as a piece of metal wire). They were selected because each has been used in hydrolysis [26] and electro-oxidation [22].

In the present study and unlike in common practices [26], our objective was not to develop an active (or very active) hydrolysis catalyst. Our objective was to work with a lowly active catalyst so that the kinetics of H$_2$ production remains slow when analyzing the solutions by ^{11}B NMR spectroscopy. We thus focused on metals in bulk state, which is a state that offers the desired catalytic activity. We ensured this by performing a series of hydrolysis experiments. Typically, 2 mL of the aforementioned alkaline solution of BH$_4^-$

(corresponding to 50 mg of NaBH$_4$) were put into contact with 16 mg of Pd, 14.5 mg of Pt, or 14.3 mg of Au at 30 °C. Regardless of the nature of the metal, it took 2 h to produce <1.6 mol H$_2$ per mol BH$_4^-$ (Figure 1), that is, <53 mL H$_2$ (out of 132 mL for a conversion of 100%). This means a H$_2$ generation rate of <0.45 mL(H$_2$) min^{-1} that is in agreement with our need. We also ensured that, in the absence of any metal, the alkaline solution of BH$_4^-$ was quite stable. At 30 °C, <0.1 mol H$_2$ per mol BH$_4^-$ was produced in 2 h (namely, <3 mL(H$_2$)).
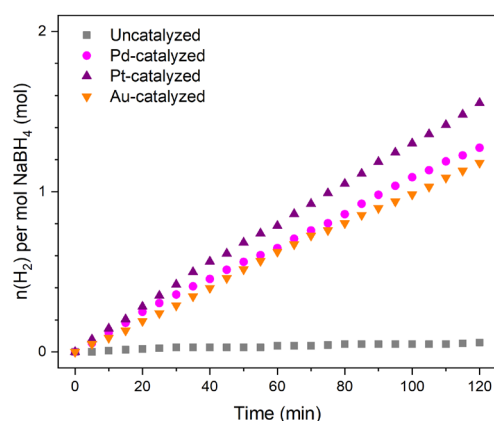

Figure 1. H$_2$ evolution curve for the hydrolysis of 2 mL of an aqueous alkaline (0.1 M NaOH) solution of BH$_4^-$ (0.66 M; i.e., 50 mg NaBH$_4$ in 2 mL) catalyzed by 16.1 mg of Pd, 14.5 mg of Pt, or 14.3 mg of Au at 30 °C. The H$_2$ evolution curve for the uncatalyzed hydrolysis test is also shown. The *y*-axis has been limited to the range 0–2 for clarity.

The hydrolysis tests were repeated to analyze the solution by ^{11}B NMR spectroscopy every hour. Similar to a previous study [13], we detected only three signals (examples of spectra in Figure 2; Table 1). The first main signal was a quintet at δ −41.5 ppm due to BH$_4^-$. The second main signal was a singlet at δ +1.9 ppm evidencing the formation of B(OH)$_4^-$ (Equation (1)). There was an additional minor and almost negligible signal, a quartet at δ −12.8 ppm. It was ascribed to the short-living intermediate BH$_3$OH$^-$ [10,15,27].
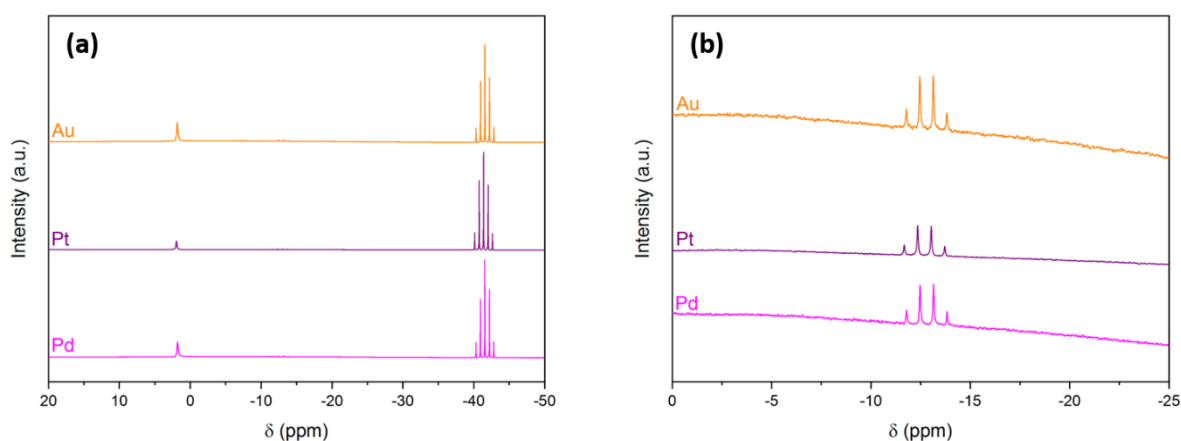

Figure 2. ^{11}B NMR spectra of the aqueous alkaline (0.1 M NaOH) solution of BH$_4^-$ (0.66 M; i.e., 50 mg NaBH$_4$ in 2 mL) upon H$_2$ evolution catalyzed by Pd, Pt, or Au at 30 °C. (**a**) Range between δ +20 and δ −50 ppm. (**b**) Focus on the range between δ 0 and −25 ppm.

Table 1. Chemical shifts (δ, in ppm) of the signals observed for the following three experiments: (a) hydrolysis conditions where H_2O acts as both reactant and solvent; (b) hydrolysis conditions where H_2O is only a reactant and DMF is used as solvent; (c) hydrolysis conditions where DMF is the solvent and H_2O is a reactant in excess. I_1 to I_3 indicates the intermediates associated to the quartets observed in the spectra collected for the experiment (c).

Experiment	$B(OH)_4^-$	I_1	BH_3OH^-	I_2	I_3	BH_4^-
(a)	+1.9		−12.8			−41.5
(b)			−14.1			−39.7
(c)		−8.9	−14.4	−20.3	−21.8	−40.5

No additional ^{11}B NMR signals that would be attributed to other short-living intermediates were seen. This might be explained by concentrations that are below the detection limit (ca. 1×10^{-3} mol L^{-1}) of the spectrometer. This might be also explained by low symmetry of the intermediates' structures, which would lead to broad signals of very low intensity and thus indistinguishable from the base line. It is worth mentioning that we used Gaussian 09 software to perform geometry optimization and NMR calculations for a series of possible intermediates including $BH_2(OH)_2^-$ and $BH(OH)_3^-$. We found that the signals of $BH_2(OH)_2^-$ and $BH(OH)_3^-$ should be a triplet and a doublet appearing between δ −7 and δ 0 ppm, respectively.

Another possible explanation of the absence of additional ^{11}B NMR signals is that the experimental conditions were not suitable for detecting intermediates with a lifetime that is shorter than that of the detected BH_3OH^-. Based on our observations, we can state that the lifetime scale of BH_3OH^- is of tens of seconds, whereas it might be much shorter (e.g., microseconds scale) for the other intermediates. Yet, the hydrolysis tests described above were performed in the presence of an excess of water: we used 2 mL (mol ratio H_2O/BH_4^- of 84) whereas about 0.1 mL (mol ratio H_2O/BH_4^- of 4) would be enough to totally hydrolyze BH_4^-. Water acted as both reactant and solvent, and the excess of water could be a favorable context to promote extremely fast hydrolysis of short-living intermediates.

2.2. Hydrolysis Conditions Where H_2O Is Only a Reactant

In order to move away from the conditions using water as both reactant and solvent, we drew on two ancient reports dealing with hydrolysis of BH_4^-. Modler and Kreevoy investigated the hydrolysis of BH_4^- (0.002 M) in moist acetonitrile (i.e., containing 0.6 M H_2O) [28], and Taub et al. used aqueous dimethylformamide (DMF) [29]. We thus selected DMF as aprotic solvent of $NaBH_4$ and used H_2O as reactant only.

We prepared four 10 mL DMF solutions of BH_4^- by dissolving 0.5 g of $NaBH_4$ (1.32 M). A piece of the aforementioned Pd, Pt, and Au was added in each of three of the DMF solutions. The fourth DMF solution was kept metal-free and is denoted uncatalyzed. We then added 0.95 mL of alkaline (0.1 M NaOH) aqueous solution to each of the four DMF solutions (resulting in a concentration of H_2O in DMF of 5.291 M). In these conditions, the mol ratio H_2O/BH_4^- was about four as for the stoichiometric hydrolysis reaction (Equation (1)). The as-prepared solutions were analyzed by ^{11}B NMR spectroscopy. It is worth mentioning that in such conditions, the hydrolysis was expected to be slow. Accordingly, the solutions were analyzed every 24 h for 3 days.

The ^{11}B NMR spectra focusing on the δ range varying from +20 to −50 ppm (Figure S1) showed only the quintet at δ −39.7 ppm due to BH_4^-. By zooming over the δ range varying from +20 to −30 ppm (Figure S2), it was possible to distinguish an additional signal of very small intensity at δ −14.1 ppm, namely the quartet due to BH_3OH^-. The quartet could be seen after 24 h for the Pd-, Pt-, and Au-catalyzed solutions, and after 48 h for the uncatalyzed solution. These results highlighted that, in the stoichiometric conditions, the hydrolysis took place to a negligible extent. Another observation is that, even in the absence of a metal, hydrolysis spontaneously took place. The non-detection of $B(OH)_4^-$ may have

up to three explanations: the amount of H_2O was too low and the H_2O molecules were very diluted in DMF, which hindered interaction-reaction with BH_4^- and BH_3OH^-; borates including $B(OH)_4^-$ were practically insoluble in DMF [30] and may have precipitated; and/or, the concentration of $B(OH)_4^-$ was below the detection limit.

2.3. Hydrolysis Conditions Where H_2O Is a Reactant in Excess

We therefore repeated the experiments while increasing the water content: the mol ratio H_2O/BH_4^- passed from 4 to 32. Once more, we prepared four 10 mL DMF solutions of BH_4^- (1.32 M) and added 7.6 mL of alkaline (0.1 M NaOH) aqueous solution. In comparison to the experiments presented in Section 2.1, the present series used water to a lesser extent (i.e., mol ratio H_2O/BH_4^- of 32 versus 84) and the 32 equivalents of H_2O were dispersed in 10 mL of DMF, mitigating the hydrolysis of BH_4^-.

As before, the ^{11}B NMR spectra (Figure S3) mainly showed the quintet at δ −40.5 ppm due to BH_4^-, and $B(OH)_4^-$ was not observed because of the reasons listed at the end of the previous section. In contrast to the results discussed above, the ^{11}B NMR spectra showed additional signals at $\delta < 0$ (Figure 3). This is discussed hereafter.
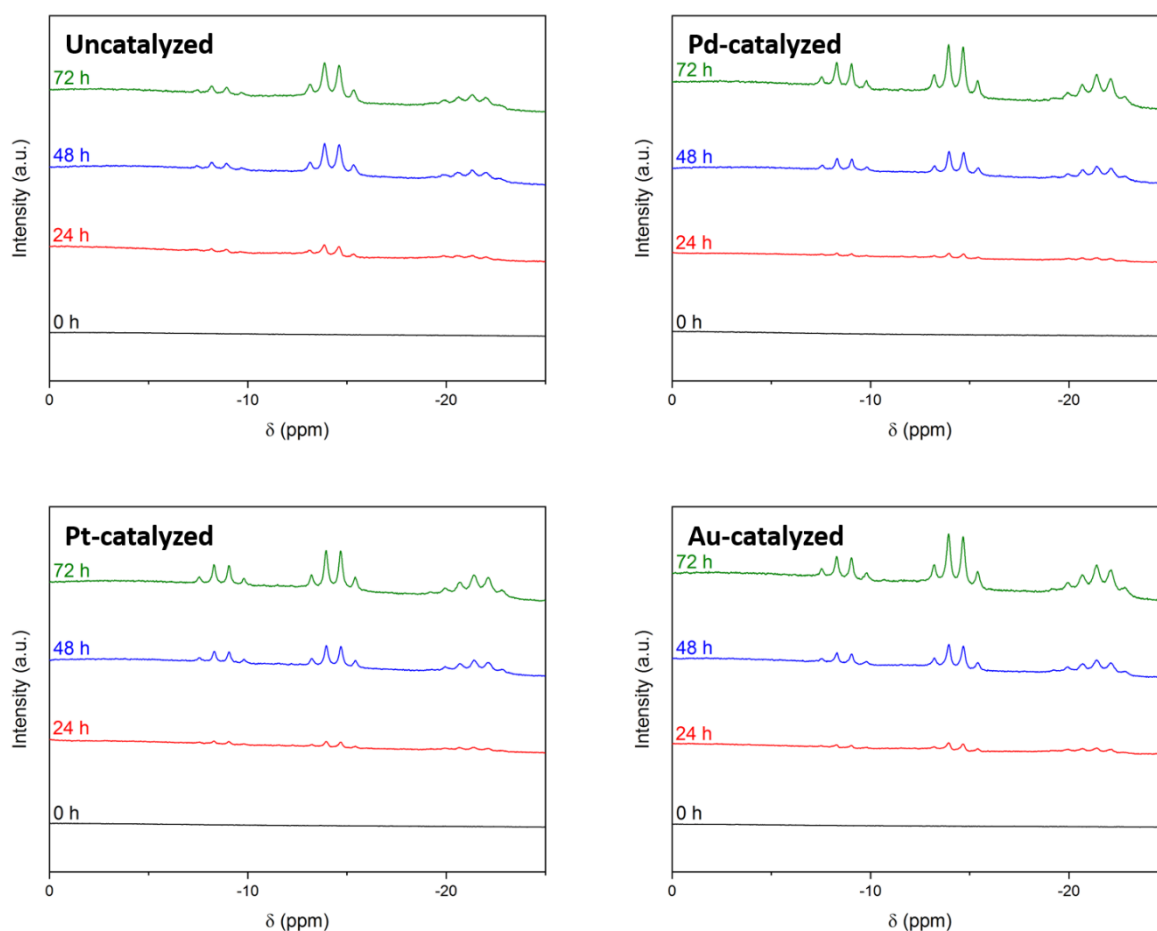

Figure 3. ^{11}B NMR spectra of the 10 mL DMF solutions of BH_4^- (1.32 M) hydrolyzed by 7.6 mL of alkaline (0.1 M NaOH), uncatalyzed or catalyzed by Pd, Pt, or Au after 0, 24, 48 and 72 h. These spectra focus on the range between δ 0 ppm and δ −25 ppm to show the signals at $\delta < 0$ ppm.

The first of the additional signals was a quartet at δ −14.4 ppm. As for our experiments discussed above, it was ascribed to BH_3OH^-.

The second of the additional signals was also a quartet, centered at δ −8.9 ppm. It indicated the formation of another BH_3-containing intermediate.

The third of the additional signals appeared as a multiplet located between δ −18.5 ppm and δ −23.5 ppm. With the help of ^{1}H-decoupled ^{11}B NMR spectroscopy, we shed light on its nature. It was the result of two distinct signals peaking at δ −20.3 ppm and δ −21.8 ppm (Figure 4). By deconvolution of the signal, we found that the two signals were more likely to be two overlapping quartets, thereby indicating the formation of two other BH_3 intermediates (Figure S4 and Table S1).
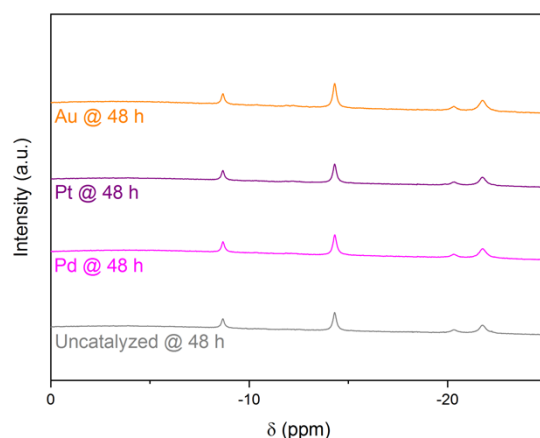

Figure 4. Proton-decoupled ^{11}B NMR of the 10 mL DMF solutions of BH_4^- (1.32 M) hydrolyzed by 7.6 mL of alkaline (0.1 M NaOH), uncatalyzed or catalyzed by Pd, Pt, or Au after 72 h.

To summarize the above: the hydrolysis of DMF-solubilized BH_4^- in the presence of 32 equivalents of H_2O involved more intermediates than the only short-living intermediate BH_3OH^-. There were three additional intermediates and they all showed a quartet in ^{11}B NMR spectroscopy, indicating that they all were made up of the BH_3 group.

We therefore focused our efforts on attributing the aforementioned quartets to possible BH_3 intermediates. We thought about any species likely to form in our conditions while exploring the open literature [31–34]. The following ones were listed (Figure 5):

- The complex $H_2O\cdot BH_3$ because H_2O is a Lewis base able to complex the Lewis acid BH_3;
- The complex $DMF\cdot BH_3$ because DMF is Lewis bases able to complex BH_3;
- The anion BH_3OH^-;
- The anion $B_2H_7^-$ (i.e., $[H_3B-H-BH_3]^-$ or $[H_4B-BH_3]^-$); and
- The pentacoordinate $BH_3(H_2)$.

According to Tague and Andrews [34], the last species $BH_3(H_2)$ possibly acts as intermediate before the formation of BH_3OH^- by reaction of BH_4^- and H_2O.

We then used Gaussian 09 software to perform geometry optimization and NMR calculations for each of these possible intermediates. We found the chemical shifts listed in Table 2. As observed in this table, a relatively good agreement between CASTEP and Gaussian 09 results was obtained considering the two investigated functionals (B3LYP for Gaussian 09 and PBE for CASTEP), except for $BH_3(H_2)$. In the case of this species, the impact of the dispersion could be invoked but additional calculations using DFT-D in CASTEP showed a very small influence of dispersion on the calculations. It is worth mentioning that in a previous study [31], the chemical shift of $B_2H_7^-$ in THF as solvent was reported to be δ −26 ppm. Similarly, using CASTEP calculations, we found comparable values (Table 2). We also calculated the chemical shifts for the intermediates based on $BH_{4-x}(OH)_x^-$ (with x = 1, 2, 3, 4), such as: BH_4^- with δ −51.5 ppm; BH_3OH^- with δ −11.4 ppm; $BH_2(OH)_2^-$ with δ +0.1 ppm; $BH(OH)_3^-$ with δ +1.1 ppm; and $B(OH)_4^-$ with δ +3.1 ppm.
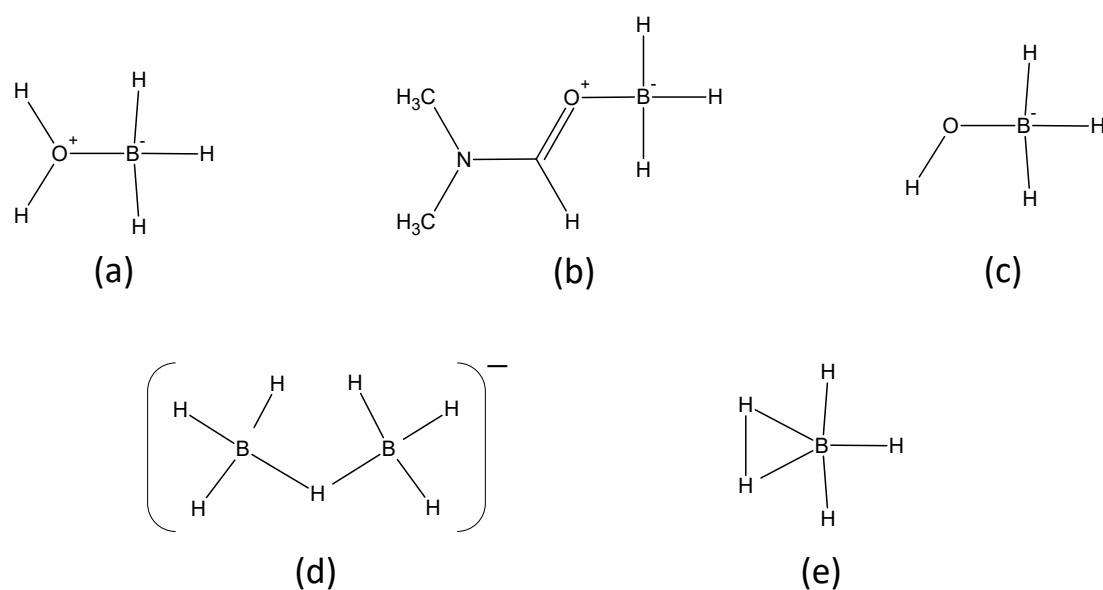
Figure 5. Possible BH_3 intermediates showing a quartet in ^{11}B NMR: (**a**) $H_2O \cdot BH_3$, (**b**) $DMF \cdot BH_3$, (**c**) BH_3OH^-, (**d**) $B_2H_7^-$, and (**e**) $BH_3(H_2)$.

Table 2. Chemical shifts (δ, in ppm) for the hypothetic BH_3-based short-living intermediates plus that of BH_4^- for comparison as calculated using Gaussian 09 and CASTEP. The experimental values for the experiment (c) are recalled, where I_1 is proposed to be $DMF \cdot BH_3$, and I_2 to be $B_2H_7^-$.

Calculation	$H_2O \cdot BH_3$	$DMF \cdot BH_3$	BH_3OH^-	$B_2H_7^-$	$BH_3(H_2)$	BH_4^-
Gaussian 09	0	−6.3	−16.8	−29.7	−40.2	−54.7
CASTEP	+2	−8.2	−11.4	−31.8	−48.1	−51.5
Experim. (c)		−8.9	−14.4	−20.3		−40.5

Going back to the results presented in Figure 3 and using the data in Table 2, we ascribed the quartets at follows. The signals at δ −8.9 ppm and δ −14.4 ppm (Figure 3) were unambiguously attributed to $DMF \cdot BH_3$ and BH_3OH^-. Because the calculated chemical shift of $BH_3(H_2)$ is much different from that of remaining signals at around δ −21 ppm, we discarded its formation. We also discarded the formation of $H_2O \cdot BH_3$ due to the absence of signals at around 0 ppm in our experimental conditions. Accordingly, the partly overlapping quartets are at δ −20.3 ppm and δ −21.8 ppm and are attributed to $B_2H_7^-$ and $B_2H_7^-$ in interaction with H_2O. Indeed, the chemical shift for the quartet due to $[B_2H_7 \cdot H_2O]^-$ was calculated as −28.1 ppm using Gaussian 09 and −32.6 ppm using CASTEP; these shifts were close to those calculated for $B_2H_7^-$ (Table 2).

Based on the experimental results reported above and supported by the calculations performed, we suggest that the BH_4^- anions dissolved in DMF are able to react with H_2O taken in excess to form BH_3-based intermediates such as $DMF \cdot BH_3$, BH_3OH^-, and $B_2H_7^-$. These intermediates are much likely to be in equilibrium. Based on the discussions reported in [30], we thus suggest that in DMF, BH_3OH^- forms first and $DMF \cdot BH_3$ and $B_2H_7^-$ forms from BH_3OH^- (by substitution of Lewis bases). This is illustrated in Figure 6.
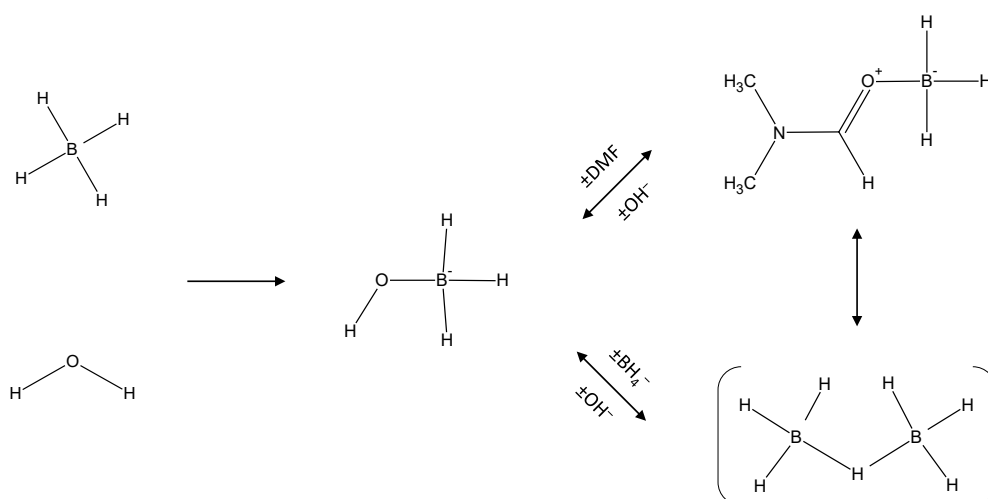
Figure 6. Mechanistic sequence illustrating the formation of the identified BH_3-based intermediates BH_3OH^-, $DMF \cdot BH_3$, and $B_2H_7^-$.

3. Materials and Methods

Sodium borohydride $NaBH_4$ (99%), sodium hydroxide NaOH ($\geq$98%), *N,N*-dimethyl formamide C_3H_7NO (DMF; 99.8%, anhydrous), Pt wire (99.9%, Ø 1.0 mm), Pd wire (99.9%, Ø 1.0 mm), and Au wire (99.95%, Ø 1.0 mm) all from Sigma-Aldrich were used as received. We stored and handled them in our argon-filled glove box (MBraun M200B, with $O_2/H_2O <$ 0.1 ppm). We used Milli-Q deionized water (18.2 MΩ cm) and it was degassed by bubbling argon for 30 min before its use.

In a first step, the hydrolysis conditions were such that water acted as both reactant and solvent. The H_2 evolution experiments were performed as follows. Under argon, 50 mg of $NaBH_4$ were transferred in a Schlenk tube (used as hydrolysis reactor). For the catalyzed experiments, a piece of metal wire (16.1 mg of Pd, 14.5 mg of Pt, or 14.3 mg of Au) was also transferred in the tube. The tube was sealed and the glove box was taken out, installed to our hydrolysis set-up (reactor connected to an inverted burette via a cold trap kept at 0 °C), and immersed in an oil bath at 30 °C. The hydrolysis reaction was started by injecting 2 mL of an aqueous alkaline (0.1 M NaOH) solution. In these conditions, the mol ratio H_2O/BH_4^- was 84. The displacement of the blue-colored liquid in the inverted burette due to the generated H_2 was video monitored. The H_2 evolution experiments were repeated to analyze the solution by ^{11}B NMR spectroscopy (Bruker Avance 400 NMR spectrometer equipped with a BBOF probe; $BF_3 \cdot OEt_2$ as reference; acetonitrile-d_3 such as $\geq$99.8 atom % D and from Sigma-Aldrich).

In a second step, the hydrolysis conditions were modified such that water only acted as reactant. To do so, 10 mL of DMF was used as solvent of 50 mg of $NaBH_4$. To this solution prepared under argon, a piece of metal was added to catalyze the reaction. The hydrolysis reaction was started by injecting 0.95 mL of alkaline (0.1 M NaOH) aqueous solution. The concentration of H_2O in DMF was 5.291 M and the mol ratio H_2O/BH_4^- was about 4. The solutions were analyzed by ^{11}B NMR spectroscopy every 24 h for 3 days.

In a third step, the hydrolysis conditions were once again modified. They were such that the water amount in DMF was increased and the mol ratio H_2O/BH_4^- passed from 4 to 32. Otherwise, the solutions were prepared similarly and they were analyzed by ^{11}B NMR spectroscopy every 24 h for 3 days.

We finalized the attribution of the ^{11}B NMR signals using theory and calculations. We used Gaussian 09 software to perform geometry optimization, vibrational analysis, and the NMR calculations. The molecular structures were determined by density functional theory calculations. A gas phase geometry optimization of the Gibbs free energy was calculated using B3LYP hybrid density functional with 6-311(++)G(2d,p) basis set at 298.15 K. NMR spectra (NMR references: TMS and BF_3-OEt$_2$) were predicted by using the same level of

theory (B3LYP/6-311++G(2d,p)). Additional computational methods were used to probe the structural properties of the different intermediates (Figure 5 and Table 2). As the reactions are difficult to stop, to isolate the structures, molecular simulations appeared to be the most powerful strategy to determine the corresponding spectroscopic properties. In complement of Gaussian 09 calculations to determine the NMR chemical shifts, calculations consisting into geometry optimization and NMR properties determination were performed using CASTEP implemented in Materials Studio 2020 [35]. This is a DFT-based code using the projector-augmented waves (PAW) and gauge-included projector-augmented waves (GIPAW) algorithms for NMR chemical shifts, respectively. Here, the PBE functional was used in the generalized gradient approximation (GGA) for the exchange correlation energy. The core−valence interactions were described by norm-conserving pseudopotentials within the NMR CASTEP package and without implementation of any additional corrections. A kinetic energy cut-off was considered and the size of the box was fixed at 10 Å (additional calculations have been performed by considering a box size fixed at 20 Å and leading to similar results), which produced converged results for geometry optimization and NMR shielding determination. The convergence of the self-consistent field (SCF) calculations were reached when the total energy variation of the system was lower than 10^{-5} eV/atom, the maximum force variation was lower than 0.03 eV/Å, and the maximal displacement was lower than 0.001 Å. In order to compare the GIPAW calculated ^{11}B shielding values with the corresponding experimental values, the following expression was used: $\delta_{\text{iso, calc}} = \sigma_{\text{ref}} - \sigma_{\text{iso}}$, where σ_{ref} corresponds to the value obtained for ^{11}B (BH$_3$-OEt$_2$) and σ_{iso} is the computational value for the investigated species.

Additional calculations were performed with CASTEP to investigate the effect of the dispersion (by considering DFT-D corrections (suing OBS method implemented in Materials Studio)) and the use of ultrasoft pseudo-potentials. A small influence on the NMR properties was observed if the dispersion was taken into account, while the use of ultrasoft pseudo-potentials led to stronger variations.

4. Conclusions

When hydrolysis of BH$_4^-$ took place in water that acted as both solvent and reactant, only one short-living intermediate was detected. It was the well-known BH$_3$OH$^-$. In such conditions, the amount of water was excessive, offering a favorable environment to the complete hydrolysis of each BH$_4^-$ into B(OH)$_4^-$. When hydrolysis of BH$_4^-$ took place in DMF in the presence of a stoichiometric amount of water, only BH$_3$OH$^-$ was detected again. In these conditions, the amount of water was too low and, if any, the other intermediates were not detected because of too low concentrations (below the detection limit). When hydrolysis of BH$_4^-$ took place in DMF as solvent and in the presence of an excess of water, four BH$_3$-based intermediates were detected, as evidenced by ^{11}B NMR quartets peaking at δ −8.9, δ −14.4, δ −20.3, and δ −21.8 ppm. Using geometry optimization and calculations, these signals could be ascribed to DMF·BH$_3$, BH$_3$OH$^-$, and B$_2$H$_7^-$ (in two conformations or in interaction with DMF or H$_2$O) that are likely to be equilibrium. This illustrates the capacity of the Lewis acid BH$_3$ to interact with Lewis bases such as DMF, OH$^-$, and BH$_4^-$. We also suggest that in DMF, BH$_3$OH$^-$ forms first and DMF·BH$_3$ and B$_2$H$_7^-$ forms from BH$_3$OH$^-$. These findings are important from a fundamental point of view for a better understanding of hydrolysis of BH$_4^-$ at the molecular level. These findings are also important for a better understanding of production of boron-based impurities in synthesis of boranes; boranes can be produced from BH$_4^-$ in an organic solvent like DMF that may contain traces of moisture.

alyzed by Pd, Pt, or Au after 0, 24, 48, and 72 h. These spectra focus on the range between δ +20 ppm and δ −30 ppm; Figure S3: ^{11}B NMR spectra of the 10 mL DMF solutions of BH_4^- (1.32 M) hydrolyzed by 7.6 mL of alkaline (0.1 M NaOH), uncatalyzed or catalyzed by Pd, Pt, or Au after 0, 24, 48, and 72 h. These spectra focus on the range between δ +20 ppm and δ −50 ppm; Figure S4: Deconvolution of the multiplet located between δ −18.5 ppm and δ −23.5 ppm for the ^{11}B NMR spectrum of the 10 mL DMF solutions of BH_4^- (1.32 M) hydrolyzed by 7.6 mL of alkaline (0.1 M NaOH) and catalyzed by Au after 48 and 72 h; Table S1: Results of the deconvolution made for the signal shown in Figure S4. The chemical shifts, Pascal's triangles, and convergences are shown; the mol files of the structures are presented in Figure 5.

Author Contributions: Conceptualization, U.B.D.; methodology, D.A. and E.P.; software, F.S. and E.P.; validation, E.P., F.S. and U.B.D.; formal analysis, E.P.; investigation, D.A.; writing—original draft preparation, U.B.D. and F.S.; writing—review and editing, E.P., F.S. and U.B.D.; supervision, U.B.D.; project administration, U.B.D. All authors have read and agreed to the published version of the manuscript.

Conflicts of Interest: The authors declare no conflict of interest.

References

1. Wee, J.H. A comparison of sodium borohydride as a fuel for proton exchange membrane fuel cells and for direct borohydride fuel cells. *J. Power Sources* **2006**, *155*, 329–339. [CrossRef]
2. Jung, E.S.; Kim, H.; Kwon, S.; Oh, T.H. Fuel cell system with sodium borohydride hydrogen generator for small unmanned aerial vehicles. *Int. J. Green Energy* **2018**, *15*, 385–392. [CrossRef]
3. Sljukic, B.; Santos, D.M.F. Direct borohydride fuel cells (DBFCs). In *Direct Liquid Fuel Cells–Fundamentals, Advances and Future*; Akay, R.G., Bayrakçeken, A., Eds.; Academic Press: London, UK, 2021; pp. 203–232.
4. Minkina, V.G.; Shabunya, S.I.; Kalinin, V.I.; Martynenko, V.V.; Smirnova, A.L. Stability of alkaline aqueous solutions of sodium borohydride. *Int. J. Hydrogen Energy* **2012**, *37*, 3313–3318. [CrossRef]
5. Damjanovic, L.; Majchrzak, M.; Bennici, S.; Auroux, A. Determination of the heat evolved during sodium borohydride hydrolysis catalyzed by Co$_3$O$_4$. *Int. J. Hydrogen Energy* **2011**, *36*, 1991–1997. [CrossRef]
6. Wang, C.; Wang, Q.; Fu, F.; Astruc, D. Hydrogen generation upon nanocatalyzed hydrolysis of hydrogen-rich boron derivatives: Recent developments. *Acc. Chem. Res.* **2020**, *53*, 2483–2493. [CrossRef] [PubMed]
7. Chatenet, M.; Monia-Concha, M.B.; El-Kissi, N.; Parrour, G.; Diard, J.P. Direct rotating ring-disk measurement of the sodium borohydride diffusion coefficient in sodium hydroxide solution. *Electrochim. Acta* **2009**, *54*, 4426–4435. [CrossRef]
8. Mochalov, K.N.; Khain, V.S.; Gil'manshin, G.G. A generalized scheme for the hydrolysis of the borohydride ion and diborane. *Dokl. Akad. Nauk. SSSR* **1965**, *162*, 613–616.
9. Gardiner, J.A.; Collat, J.W. Kinetics of the stepwise hydrolysis of tetrahydroborate ion. *J. Am. Chem. Soc.* **1965**, *87*, 1692–1700. [CrossRef]
10. Guella, G.; Zanchetta, C.; Patton, B.; Miotello, A. New insights on the mechanism of palladium-catalyzed hydrolysis of sodium borohydride from ^{11}B NMR measurements. *J. Phys. Chem. B* **2006**, *110*, 17024–17033. [CrossRef]
11. Lu, L.; Zhang, H.; Zhang, S.; Li, F. A family of high-efficiency hydrogen-generation catalysts based on ammonium species. *Angew. Chem. Int. Ed.* **2015**, *127*, 9460–9464. [CrossRef]
12. Zhou, Y.; Fang, C.; Fang, Y.; Zhu, F.; Liu, H.; Ge, H. Hydrogen generation mechanism of BH_4^- spontaneous hydrolysis: A sight from ab initio calculation. *Int. J. Hydrogen Energy* **2016**, *41*, 22668–22676. [CrossRef]
13. Andrieux, J.; Demirci, U.B.; Hannauer, J.; Gervais, C.; Goutaudier, C.; Miele, P. Spontaneous hydrolysis of sodium borohydride in harsh conditions. *Int. J. Hydrogen Energy* **2011**, *36*, 224–233. [CrossRef]
14. Churikov, A.V.; Gamayunova, I.M.; Zapsis, K.V.; Chrikov, M.A.; Ivanishchev, A.V. Influence of temperature and alkalinity on the hydrolysis rate of borohydride ions in aqueous solution. *Int. J. Hydrogen Energy* **2012**, *37*, 335–344. [CrossRef]
15. Choi, S.; Jeong, Y.; Yu, J. Spontaneous hydrolysis of borohydride required before its catalytic activation by metal nanoparticles. *Catal. Commun.* **2016**, *84*, 80–84. [CrossRef]
16. Budroni, M.A.; Garroni, S.; Mulas, G.; Rustici, M. Bursting dynamics in molecular Hydrogen generation via sodium borohydride hydrolysis. *J. Phys. Chem. C* **2017**, *121*, 4891–4898. [CrossRef]
17. Elder, J.P.; Hickling, A. Anodic behaviour of the borohydride ion. *Trans. Faraday Soc.* **1962**, *58*, 1852–1864. [CrossRef]
18. Elder, J.P. Hydrogen ionization in the anodic oxidation of the borohydride ion. *Electrochim. Acta* **1962**, *7*, 417–426. [CrossRef]
19. Gyenge, E. Electrooxidation of borohydride on platinum and gold electrodes: Implications for direct borohydride fuel cells. *Electrochim. Acta* **2004**, *49*, 965–978. [CrossRef]
20. Liu, B.H.; Li, Z.P.; Suda, S. Electrocatalysts for the anodic oxidation of borohydrides. *Electrochim. Act* **2004**, *49*, 3097–3105. [CrossRef]

21. Molina Concha, B.; Chatenet, M.; Coutanceau, C.; Hahn, F. In situ infrared (FTIR) study of the borohydride oxidation reaction. *Electrochem. Commun.* **2009**, *11*, 223–226. [CrossRef]
22. Braesch, G.; Bonnefont, A.; Martin, V.; Savinova, E.R.; Chatenet, M. Borohydride oxidation reaction mechanisms and poisoning effects on Au, Pt and Pd bulk electrodes: From model (low) to direct borohydride fuel cell operating (high) concentrations. *Electrochim. Acta* **2018**, *273*, 483–494. [CrossRef]
23. Olu, P.Y.; Bonnefont, A.; Braesch, G.; Martin, V.; Savinova, E.R.; Chatenet, M. Influence of the concentration of borohydride towards hydrogen production and escape for borohydride oxidation reaction on Pt and Au electrodes–experimental and modelling insights. *J. Power Sources* **2018**, *375*, 300–309. [CrossRef]
24. Molina Concha, B.; Chatenet, M.; Ticianelli, E.A.; Lima, F.H.B. In situ infrared (FTIR) study of the mechanism of the borohydride oxidation reaction on smooth Pt electrode. *J. Phys. Chem. C* **2011**, *115*, 12439–12447. [CrossRef]
25. Nanayakkara, S.; Freindorf, M.; Tao, Y.; Kraka, E. Modeling hydrogen release from water with borane and alene catalysts: A unified reaction valley approach. *J. Phys. Chem. A* **2020**, *124*, 8978–8993. [CrossRef]
26. Demirci, U.B. The hydrogen cycle with the hydrolysis of sodium borohydride: A statistical approach for highlighting the scientific/technical issues to prioritize in the field. *Int. J. Hydrogen Energy* **2015**, *40*, 2673–2691. [CrossRef]
27. Ruman, T.; Kusnierz, A.; Jurkiewicz, A.; Les, A.; Rode, W. The synthesis, reactivity and ^{1}H NMR investigation of the hydroxy-borohydride anion. *Inorg. Chem. Commun.* **2007**, *10*, 1074–1978. [CrossRef]
28. Modler, R.F.; Kreevoy, M.M. Hydrolysis mechanism of BH_4^- in moist acetonitrile. *J. Am. Chem. Soc.* **1977**, *99*, 2271–2275. [CrossRef]
29. Taub, D.; Hoffsommer, R.D.; Wendler, N.L. Selective sodium borohydride reductions in aqueous dimethylformamide solution. Neighboring group effects in the cortical side chain. *J. Am. Chem. Soc.* **1959**, *81*, 3291–3294. [CrossRef]
30. Angelova, L.V.; Terech, P.; Natali, I.; Dei, L.; Carretti, E.; Weiss, R.G. Cosolvent gel-like materials from partially hydrolyzed poly(vinyl acetate)s and borax. *Langmuir* **2011**, *27*, 11671–11682. [CrossRef]
31. Jolly, W.L.; Schmitt, T. Evidence for the species BH_2^+ and $BH(OH)_2$ in aqueous solutions. The reaction of diborane with hydroxide. *J. Am. Chem. Soc.* **1966**, *88*, 4282–4284. [CrossRef]
32. Chen, X.M.; Ma, N.; Zhang, Q.F.; Wang, J.; Feng, X.; Wei, C.; Wang, L.S.; Zhang, J.; Chen, X. Elucidation of the formation mechanisms of the octahydrotriborate anion ($B_3H_8^-$) through the nucleophilicity of the B−H bond. *J. Am. Chem. Soc.* **2018**, *140*, 6718–6726. [CrossRef] [PubMed]
33. D'Ulivo, A. The contribution of chemical vapor generation coupled with atomic or mass spectrometry to the comprehension of the chemistry of aqueous boranes. *J. Anal. At. Spectrom.* **2019**, *34*, 823–847. [CrossRef]
34. Tague, T.J.; Andrews, L. Reactions of pulsed-laser evaporated boron atoms with hydrogen. Infrared spectra of boron hydride intermediate species in solid argon. *J. Am. Chem. Soc.* **1994**, *116*, 4970–4976. [CrossRef]
35. Segall, M.D.; Lindan, P.L.D.; Probert, M.J.; Pickard, C.J.; Hasnip, P.J.; Clark, S.J.; Payne, M.C. First-principles simulation: Ideas, illustrations and the CASTEP code. *J. Phys. Condens. Matter* **2002**, *14*, 2717–2744. [CrossRef]